

Solar Activity, Magnetism, and Irradiance, SAMI18,
The conference *in honor of Sami Solanki*, Göttingen October 16–18, 2018

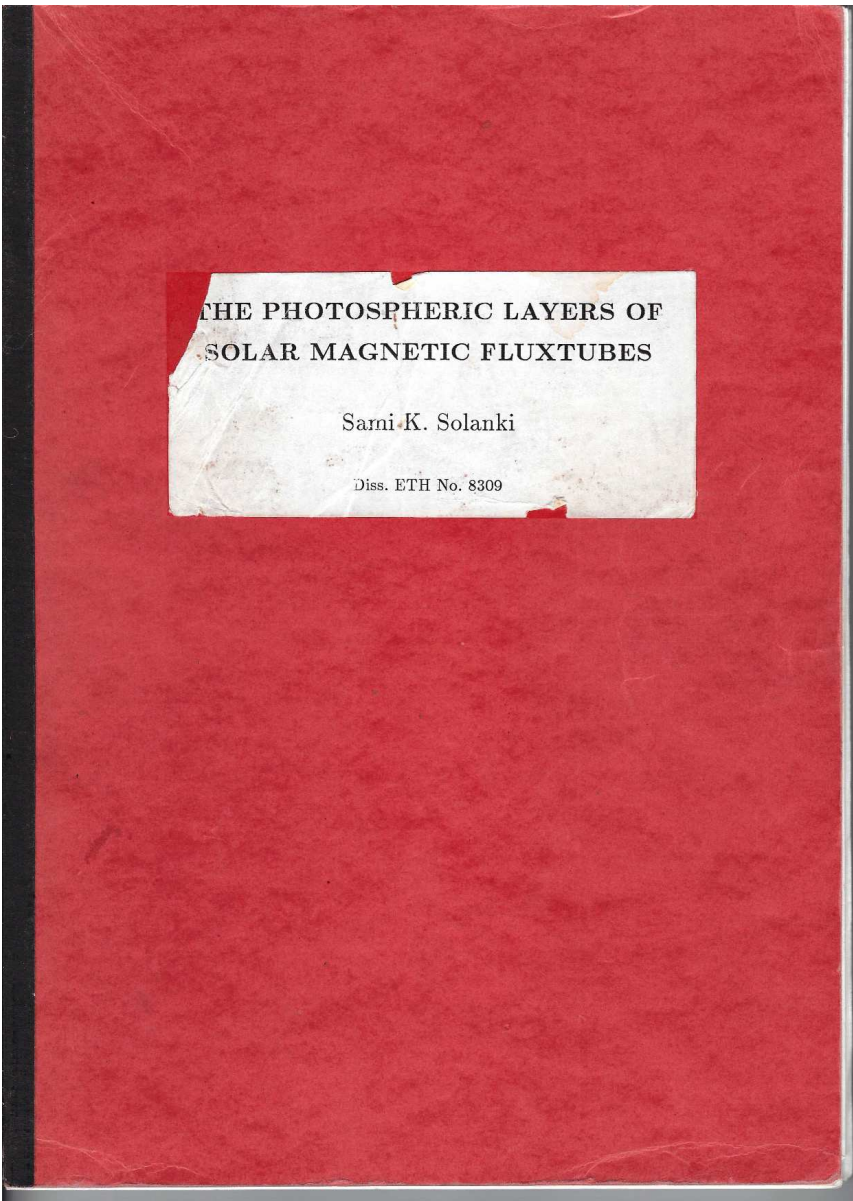
On flux tubes and irradiance: reminiscences and news

Oskar Steiner^{1,2}

¹Kiepenheuer-Institut für Sonnenphysik (KIS), Freiburg i.Br., Germany

²Istituto Ricerche Solari Locarno (IRSOL), Locarno Monti, Switzerland

1. On magnetic flux tubes



Tattered cover of my personal copy of
Sami's PhD thesis *The Photospheric
Layers of Solar Magnetic Fluxtubes.*

*Sami K. Solanki (1987), PhD thesis
ETH 8309*

On magnetic flux tubes (cont.)

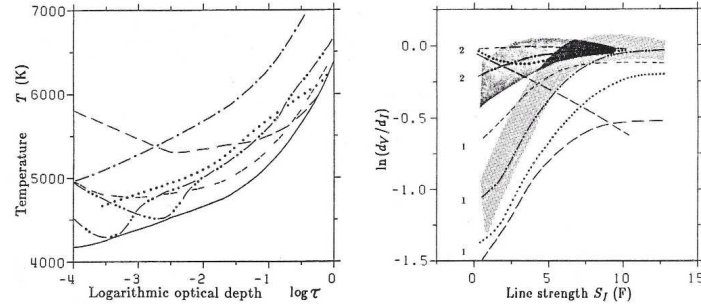
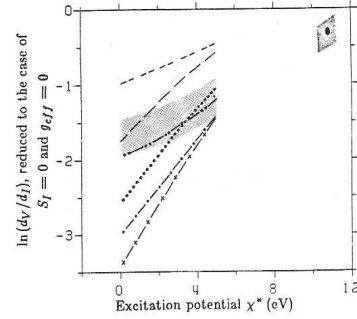


Fig. 5.8 a Temperature stratification of some empirical models of plage fluxtubes and the HSRA (solid line). Stenflo (1975): - - -, Hirayama (1978) model Z: · · · · · , Chapman (1979): — — —, Stellmacher and Wiehr (1979): — — —, Solanki (1984), model 6K: — · — · —, model 6P: — · · — · —, b $\ln(dv/d\tau)$ vs. S_I for plage data (light shading: Fe I, $x_c < 3$ eV; dark shading: Fe II), and the models listed in the caption of Fig. 5.8a. Model curves labeled '1' refer to Fe I, those labeled '2' refer to Fe II.

only one curve has been plotted. The model curves have been shifted in such a way that they all reproduce the Fe II data equally well.

Fig. 5.9 $\ln(dv/d\tau)$ reduced to $S_I = 0$ and $g_{eff} = 0$ vs. x^* for network data (light shading: Fe I, dark shading: Fe II) and the models listed in the caption of Fig. 5.7a.

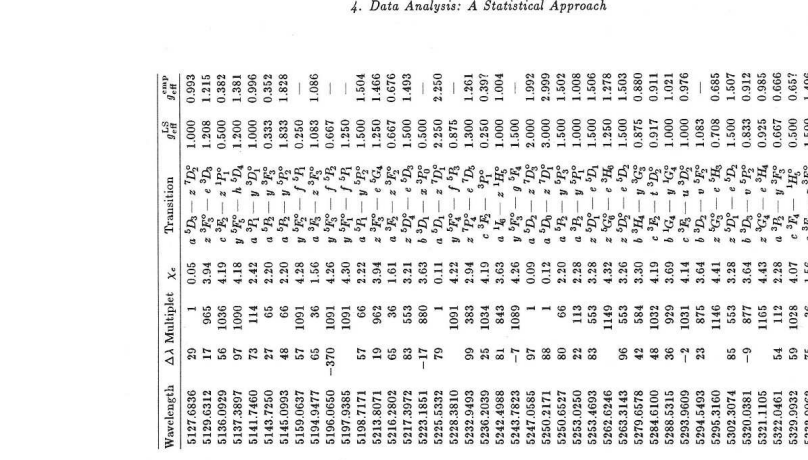


5.9.2. Discussion

In the following we list some comments on the figures and the models presented above.

- The large spread of the model curves in Figs. 5.7b and 5.8b is evidence for the temperature sensitivity of the $\ln(dv/d\tau)$ vs. S_I diagram. It also reflects the different types of data on which the various models are based. Usually the data come from more or less high spatial resolution Stokes I or continuum observations (and sometimes both), the exceptions being Stenflo (1975), who also used the Stokes V profiles of two lines, and models presented in this thesis. The models using both Stokes I and V represent just the magnetic regions

Semi-empirical atmospheres of plage and network magnetic flux tubes, also called the “*Semi-empirical*” models by Uli Grossmann-Doerth.



Wavelength	ΔΔ Multiplet	x^*	g_{eff}^{emp}	Transition
4939.6931	71	16	0.86	$a \ ^5D_0 - z \ ^5P_0$
4945.6390	25	1113	4.21	$y \ ^5D_0 - f \ ^5P_0$
4946.3941	92	687	3.37	$z \ ^5D_0 - e \ ^5P_0$
4950.1108	67	687	3.42	$x \ ^5D_0 - e \ ^5P_0$
4982.4776	205	1097	4.18	$y \ ^5D_0 - e \ ^5P_0$
4989.9328	71	1066	4.42	$y \ ^5D_0 - h \ ^5P_1$
4979.5881	71	1067	4.10	$y \ ^5D_0 - f \ ^5P_1$
4982.5063	86	1067	4.16	$y \ ^5D_0 - f \ ^5P_2$
4985.2587	73	984	3.93	$z \ ^5D_0 - f \ ^5P_2$
4986.5530	72	318	2.86	$z \ ^5D_0 - e \ ^5P_2$
4986.2252	8	1070	4.22	$y \ ^5D_0 - f \ ^5P_2$
4986.5650	99	1066	4.15	$y \ ^5D_0 - h \ ^5P_2$
4992.7870	1110	4.26	—	$x \ ^5D_0 - e \ ^5P_3$
4994.1364	76	16	0.91	$a \ ^5F_3 - g \ ^5P_3$
4995.4109	1113	4.26	—	$a \ ^5F_3 - f \ ^5P_2$
4999.1135	-6	1040	4.19	$c \ ^5G_3 - f \ ^5P_2$
5001.8760	138	1065	3.88	$z \ ^5G_3 - f \ ^5P_2$
5002.7986	92	687	3.40	$z \ ^5G_3 - e \ ^5P_2$
5012.6933	59	1093	3.94	$y \ ^5G_3 - e \ ^5H_4$
5014.0505	93	965	3.94	$y \ ^5G_3 - e \ ^5D_2$
5016.4478	22	1089	4.26	$y \ ^5G_3 - g \ ^5S$
5023.2420	67	1095	4.28	$y \ ^5G_3 - f \ ^5D_1$
5023.1870	1095	4.28	—	$y \ ^5G_3 - f \ ^5D_2$
5029.5298	-3	718	2.41	$y \ ^5D_1 - f \ ^5P_2$
5030.7807	86	1085	3.84	$b \ ^3D_1 - e \ ^3P_2$
5034.2164	59	318	2.85	$e \ ^3D_1 - e \ ^3P_2$
5048.4413	82	984	3.96	$y \ ^3D_1 - e \ ^3P_2$
5054.6457	42	884	3.64	$b \ ^3D_1 - v \ ^3P_2$
5058.4987	26	884	3.64	$b \ ^3D_1 - v \ ^3P_3$
5067.1569	61	1092	4.22	$y \ ^3D_1 - f \ ^3P_4$
5072.6767	117	1095	4.22	$y \ ^3D_1 - f \ ^3P_5$
5074.7556	77	1094	4.22	$y \ ^3D_1 - e \ ^3P_5$
5079.7462	77	16	0.90	$a \ ^3F_2 - g \ ^3P_2$
5083.3450	73	16	0.96	$a \ ^3F_2 - z \ ^3P_2$
5098.1559	57	1066	4.15	$y \ ^3P_2 - h \ ^3D_2$
5090.7807	57	1090	4.26	$y \ ^3P_2 - h \ ^3D_3$
5104.0338	47	465	3.02	$c \ ^3P_2 - w \ ^3D_2$
5104.1916	1092	4.18	—	$b \ ^3P_2 - w \ ^3D_2$
5109.6544	47	1089	4.30	$y \ ^3P_2 - g \ ^3P_2$
5127.3655	74	16	0.91	$a \ ^3P_2 - z \ ^3P_2$

One of seven pages of Fe I and Fe II lines and their Landé factors.

On magnetic flux tubes (cont.)

9.2. Basic Equations

If we neglect the transport of energy, then a magnetised gas with infinite conductivity (and a magnetic permeability of 1) in an external constant gravitational field can be described in the MHD approximation by the equation of continuity, divergence freedom of \mathbf{B} , the momentum transport equation, and the equation of state of an ideal gas

$$\frac{\partial \rho}{\partial t} + \nabla(\rho \mathbf{v}) = 0, \quad (9.1)$$

$$\nabla \cdot \mathbf{B} = 0, \quad (9.2)$$

$$\rho \frac{d\mathbf{v}}{dt} = \rho g - \nabla P + \frac{1}{4\pi} (\nabla \times \mathbf{B}) \times \mathbf{B} + \mathbf{F}, \quad (9.3)$$

$$P = \rho \mathcal{R} T / m_p, \quad (9.4)$$

where ρ is the density, \mathbf{v} the velocity vector, \mathbf{B} the magnetic field vector, g the acceleration due to gravity, \mathbf{F} the vector of the viscous force per unit volume, P the gas pressure, \mathcal{R} the universal gas constant, and m_p the mean particle mass.

For the stationary structure of a solar magnetic fluxtube in the absence of flows (cf. Sect. 7.2) we need use only the magnetohydrostatic approximation, and the above set of equations reduces to

$$\nabla \cdot \mathbf{B} = 0, \quad (9.5)$$

$$\nabla P = \frac{1}{4\pi} (\nabla \times \mathbf{B}) \times \mathbf{B} + \rho g, \quad (9.6)$$

$$P = \rho \mathcal{R} T / m_p. \quad (9.7)$$

We now assume that the fluxtube is rotationally symmetric around the vertical z -axis, i.e. we reduce the problem to two dimensions. Let r , θ , and z be ordinary cylindrical coordinates. In this geometry Eqs. (9.5) to (9.7) become

$$4\pi \frac{\partial P}{\partial r} = B_z \left(\frac{\partial B_r}{\partial z} - \frac{\partial B_z}{\partial r} \right) - \frac{B_\theta}{r} \frac{\partial}{\partial r}(r B_\theta), \quad (9.8)$$

$$0 = \frac{B_r}{r} \frac{\partial}{\partial r}(r B_\theta) + B_z \frac{\partial B_\theta}{\partial z}, \quad (9.9)$$

$$4\pi \left(\frac{\partial P}{\partial z} + \frac{P}{H} \right) = -B_r \left(\frac{\partial B_r}{\partial z} - \frac{\partial B_z}{\partial r} \right) - B_\theta \frac{\partial B_\theta}{\partial z}, \quad (9.10)$$

$$0 = \frac{1}{r} \frac{\partial}{\partial r}(r B_r) + \frac{\partial B_z}{\partial z}, \quad (9.11)$$

where B_r , B_θ , and B_z are the three components of the magnetic field, and H the scale height defined by

$$H(z) = \frac{kT(z) R_\odot^2}{G m_p M_\odot}, \quad (9.12)$$

k being Boltzmann's constant, T the temperature, R_\odot the solar radius, G the gravitational constant, and M_\odot the solar mass. Fig. 9.1 illustrates some of the basic quantities.

Further calculations are simplified by transforming Eqs. (9.8)–(9.11) into non-dimensional form. To this end we define the following non-dimensional quantities

$$x = r/H^*, \quad (9.13)$$

$$y = z/H^*, \quad (9.14)$$

$$\mathbf{b} = \mathbf{B}/B^*, \quad (9.15)$$

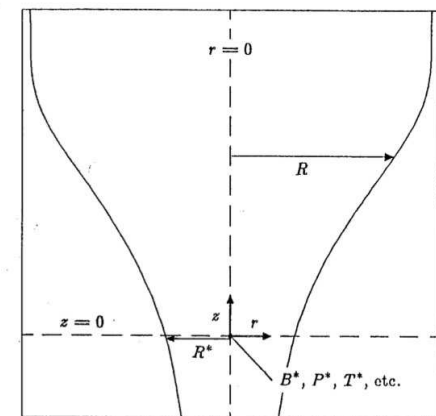
$$p = P/P^*, \quad (9.16)$$

$$\sigma = T/T^*, \quad (9.17)$$

where B^* , P^* , and T^* are the values of B , P , and T at the reference height $z = 0$ on the axis of the fluxtube (Fig. 9.1), and

$$H^* = \frac{kT^* R_\odot^2}{G m_p M_\odot}. \quad (9.18)$$

Fig. 9.1 Schematic of fluxtube geometry showing pertinent definitions.



Eqs. (9.8)–(9.11) then become

$$\beta \frac{\partial p}{\partial x} = b_z \left(\frac{\partial b_r}{\partial y} - \frac{\partial b_z}{\partial x} \right) - \frac{b_\theta}{x} \frac{\partial}{\partial x}(x b_\theta), \quad (9.19)$$

$$0 = \frac{b_r}{x} \frac{\partial}{\partial x}(x b_\theta) + b_z \frac{\partial b_\theta}{\partial y}, \quad (9.20)$$

$$\beta \left(\frac{\partial p}{\partial y} + \frac{p}{\sigma} \right) = -b_r \left(\frac{\partial b_r}{\partial y} - \frac{\partial b_z}{\partial x} \right) - b_\theta \frac{\partial b_\theta}{\partial y}, \quad (9.21)$$

$$0 = \frac{1}{x} \frac{\partial}{\partial x}(x b_r) + \frac{\partial b_z}{\partial y}, \quad (9.22)$$

where

$$\beta = 4\pi \frac{p^*}{b^{*2}}. \quad (9.23)$$

We now expand all variables in a power series in x .

$$b_z = h_0 + h_2 x^2 + h_4 x^4 + \dots, \quad (9.24)$$

$$b_r = f_1 x + f_3 x^3 + \dots, \quad (9.25)$$

$$b_\theta = g_1 x + g_3 x^3 + \dots, \quad (9.26)$$

We express b_z by an even series in x , while b_r and b_θ are given by odd series. This is consistent with power series expansions of potential fields and analytical force free fields (cf. Ferraro and Plumpton, 1966). For p and σ expansions containing only even terms are used as well, as suggested by the form of the Eqs. (9.19)–(9.22).

$$p = p_0 + p_2 x^2 + p_4 x^4 + \dots, \quad (9.27)$$

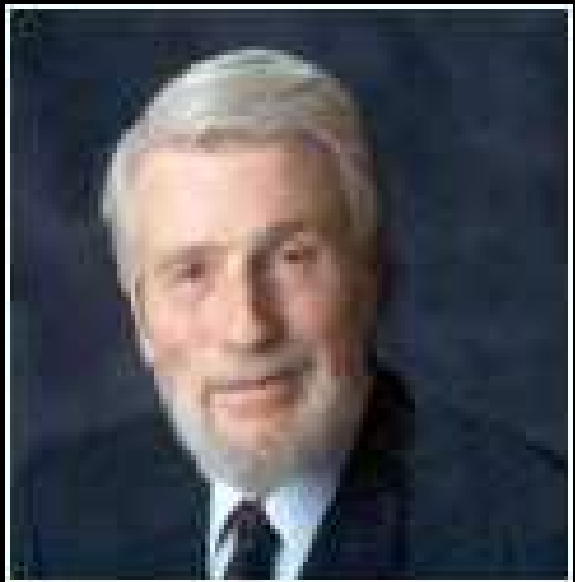
$$\sigma = \sigma_0 + \sigma_2 x^2 + \sigma_4 x^4 + \dots. \quad (9.28)$$

The gas density can be determined via the ideal gas equation (9.7) and need not concern us further in this chapter.[†] Now Equations (9.19) – (9.22) assume the form

$$2\beta(p_2 + 2p_4 x^2 + \dots) = (h_0 + h_2 x^2 + \dots)((f'_1 + f'_3 x^2 + \dots) - (2h_2 + 4h_4 x^2 + \dots)) - (g_1 + g_3 x^2 + \dots)(2g_1 + 4g_3 x^2 + \dots), \quad (9.29)$$

[†] It is not required for radiative transfer calculations either.

On magnetic flux tubes (cont.)



Gerald "Jerry" W. Pneuman, 1931–2004

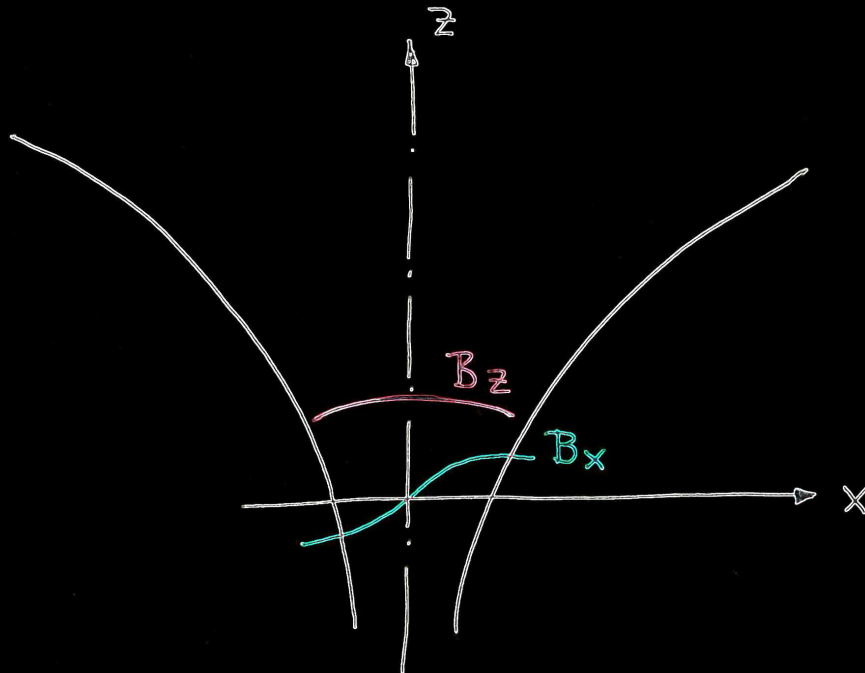
Scientist at the High Altitude Observatory from 1968 to 1987. Visiting scientist at the Institute of Astronomy at ETH from 1984 to 1985.

Work on coronal magnetic fields (coronal streamers) and space physics.

Pneuman, G.W., Solanki, S.K., and Stenflo, J.O.: 1986, *Structure and merging of solar magnetic fluxtubes*, A&A 154, 231

Steiner, O., Pneuman, G.W., and Stenflo, J.O.: 1986, *Numerical models of solar magnetic fluxtubes*, A&A 170, 126

On magnetic flux tubes



Approximate sketch by Jerry Pneuman, explaining even an odd power expansions for B_z and B_r , respectively.

Find proof in:

Ferriz Mas, A. and Schüssler, M.: 1989, *Radial expansion of the magnetohydrodynamic equations for axially symmetric configurations*, Geophys. Astrophys. Fluid Dynamics 48, 217-234

On magnetic flux tubes (cont.)

Solution of a 2nd order ODE with the help of a *shooting method*.

Sami shoots faster than Lucky Luke who already shoots faster than his own shadow.

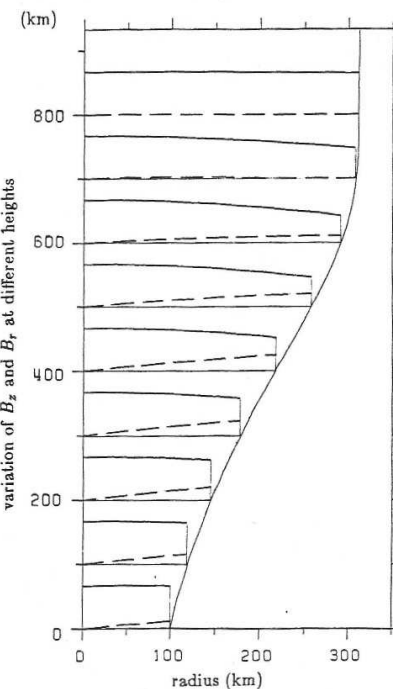
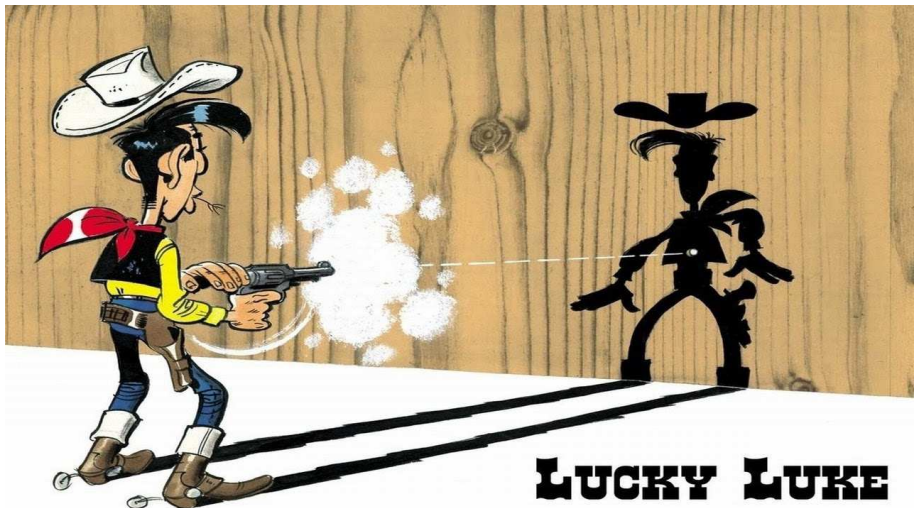


Fig. 9.6 Radial variation of B_z and B_r at different heights for a typical fluxtube of initial radius equal to 100 km and a filling factor of 0.1. For this case, the base gas pressure is taken to be uniform. To interpret this figure and others like it properly, visualize the figure of the overall fluxtube geometry to be subdivided into groups of subfigures placed at different heights in the tube. Each subfigure contains three curves. At the bottom is a horizontal line defining the height. Above it is the radial variation of B_r shown dashed and, above that, the variation of B_z (solid). As in all figures of this type, both B_z and B_r are normalized to the value of B_z on the axis. Here, the axial field at the base is essentially uniform but then begins to decline outward as the height increases. But, near the merging height, it approaches uniformity again, consistent with a uniform vertical cross-section.

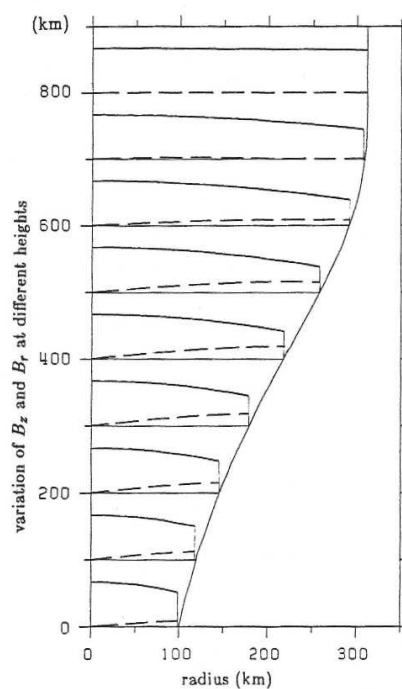
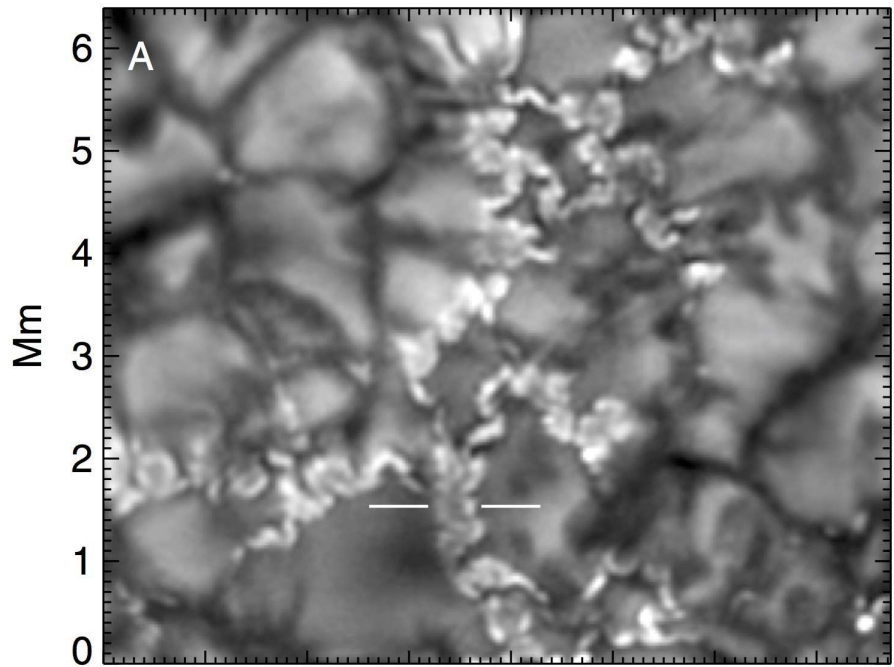


Fig. 9.7 The same as Fig. 9.6 but with a base gas pressure increasing outward from the axis. Now, the axial field is no longer uniform at the base since its pressure gradient must balance the inward gas pressure gradient. At large heights, however, the gas pressure is no longer important and the field approaches uniformity as in Fig. 9.6.

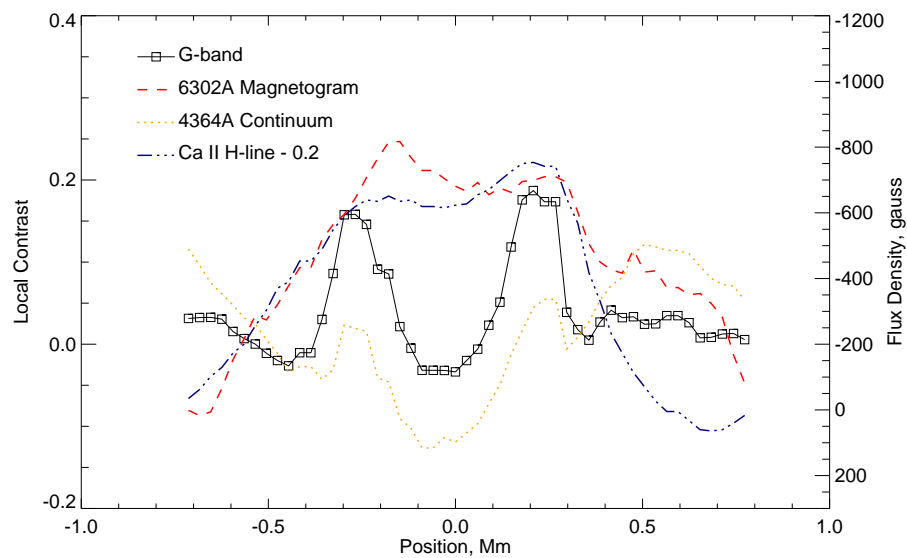
On magnetic flux tubes (cont.)



“... magnetic flux ... is typically structured into larger, amorphous, “ribbons” which are not resolved into individual flux tubes.” From *Berger et al. 2004, A&A 428, 613*.

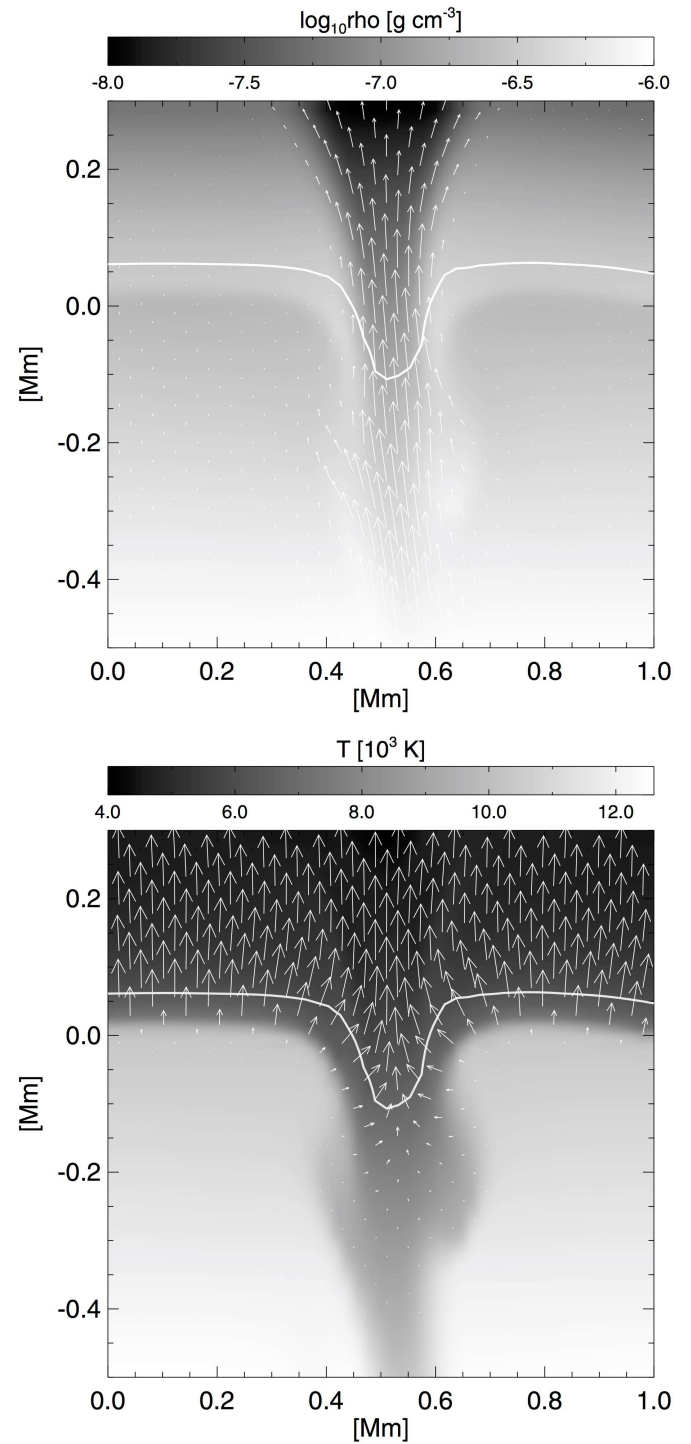
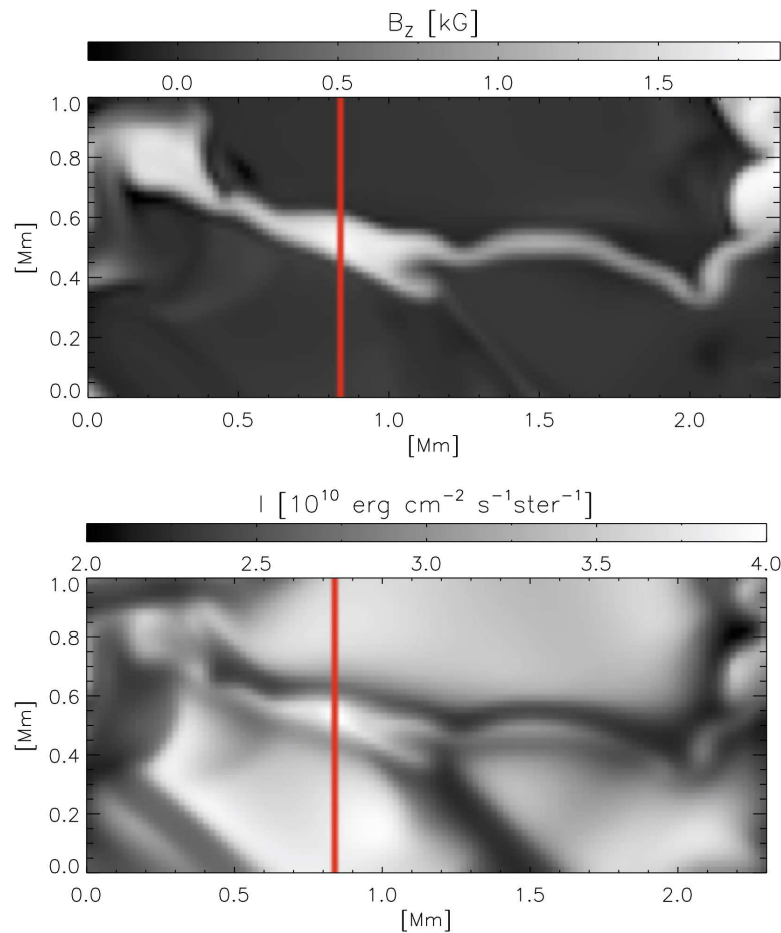
“... the time-evolution is more that of a magnetic fluid than that of collections of flux-tubes.”

From *Rouppe van der Voort et al. 2005, A&A 435, 327*.



Contrast profile and magnetic field strength of a “ribbon” structure. From *Berger et al. 2004*.

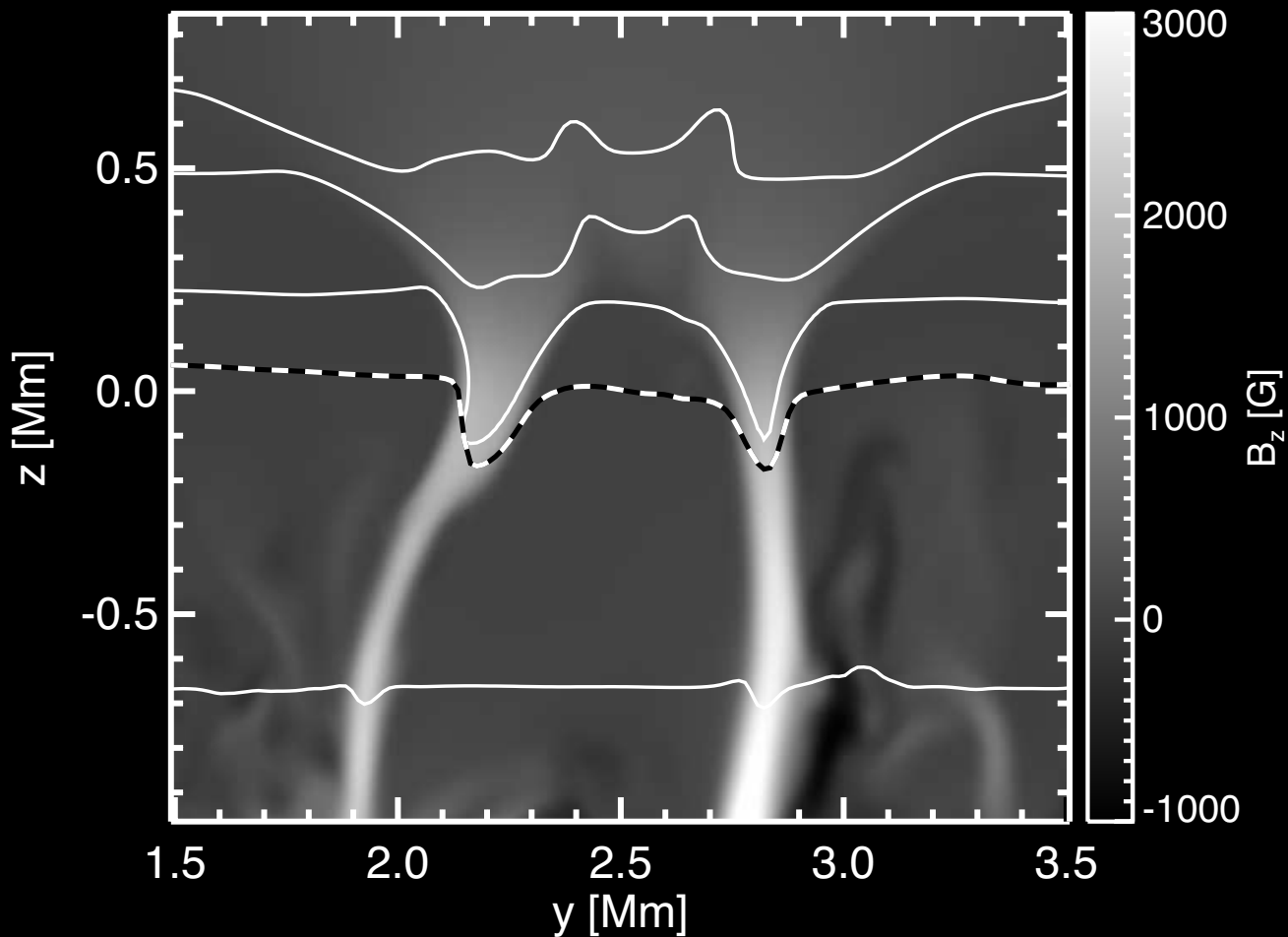
On magnetic flux tubes (cont.)



“This example ... demonstrates that results of idealized, two-dimensional models are indeed relevant for the explanation of some aspects of three-dimensional magnetoconvection.”

From *Vögler et al. 2005*.

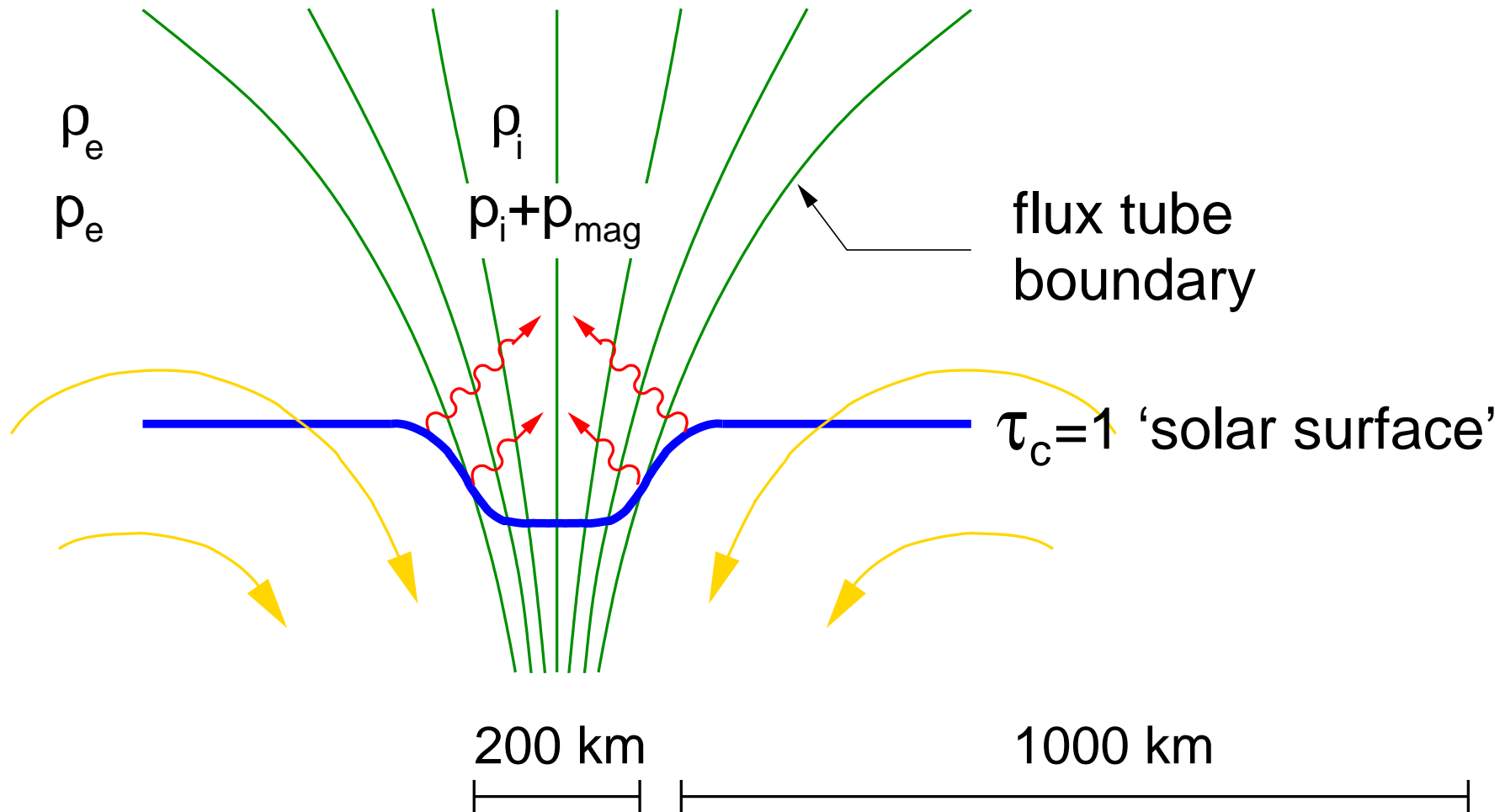
On magnetic flux tubes (cont.)



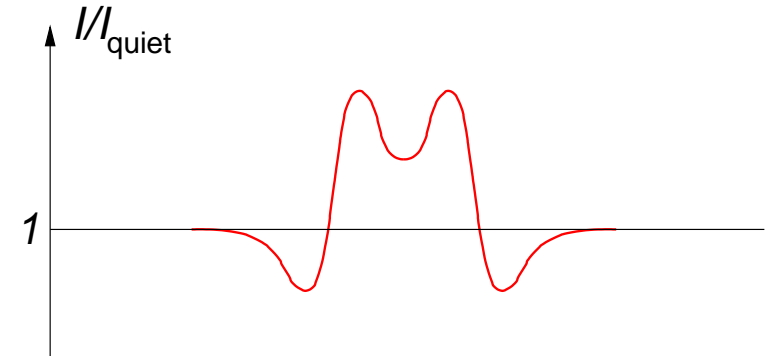
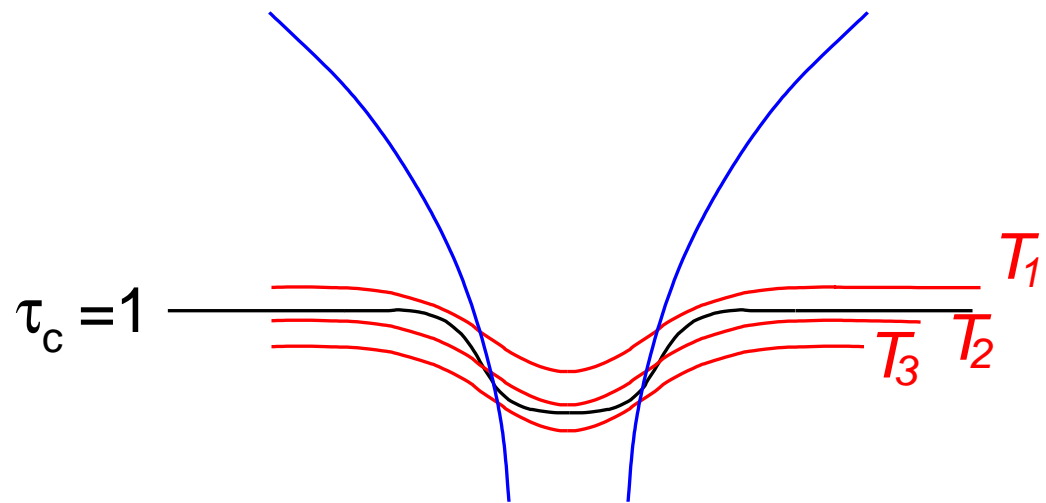
Vertical section through a CO^5BOLD simulation snapshot. *Gray scales*: vertical magnetic field strength. *Dashed curve*: $\tau_R = 1$ contour. *Solid white curves*: contours of constant density.

From *Salhab et al. 2018*.

2. On irradiance

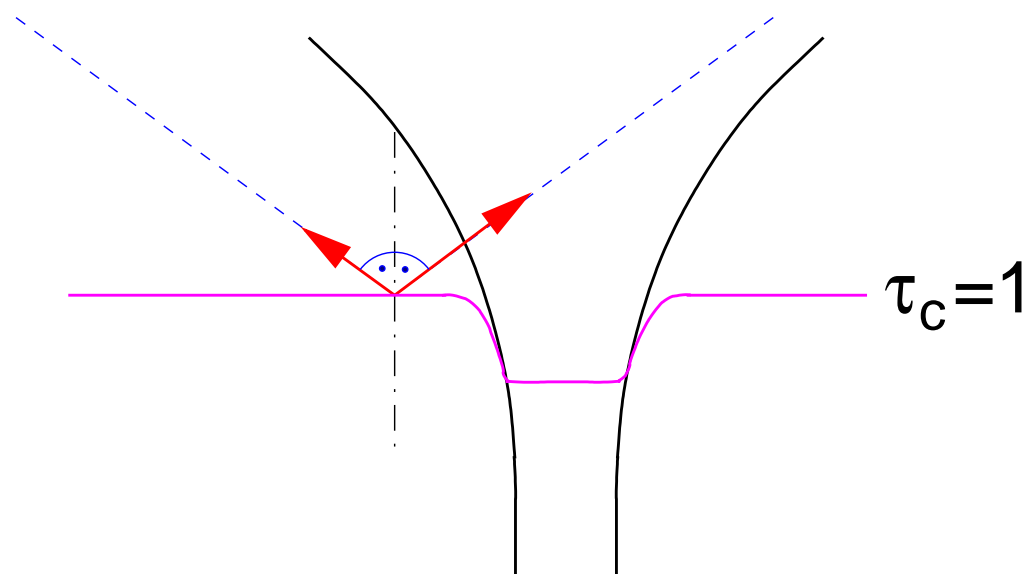


On irradiance (cont.)

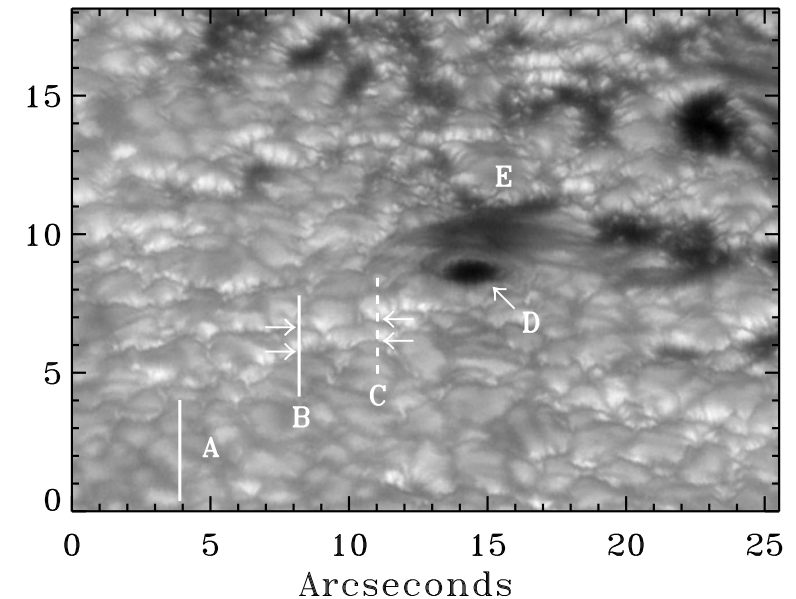


Sketch of the optical surface of $\tau_c = 1$ in relation to isothermal contours and corresponding contrast profile. Sketch derived from results of the stationary magnetohydrodynamic model of *Deinzer, Hensler, Schüssler, and Weisshaar 1984a,b*.

On irradiance (cont.)

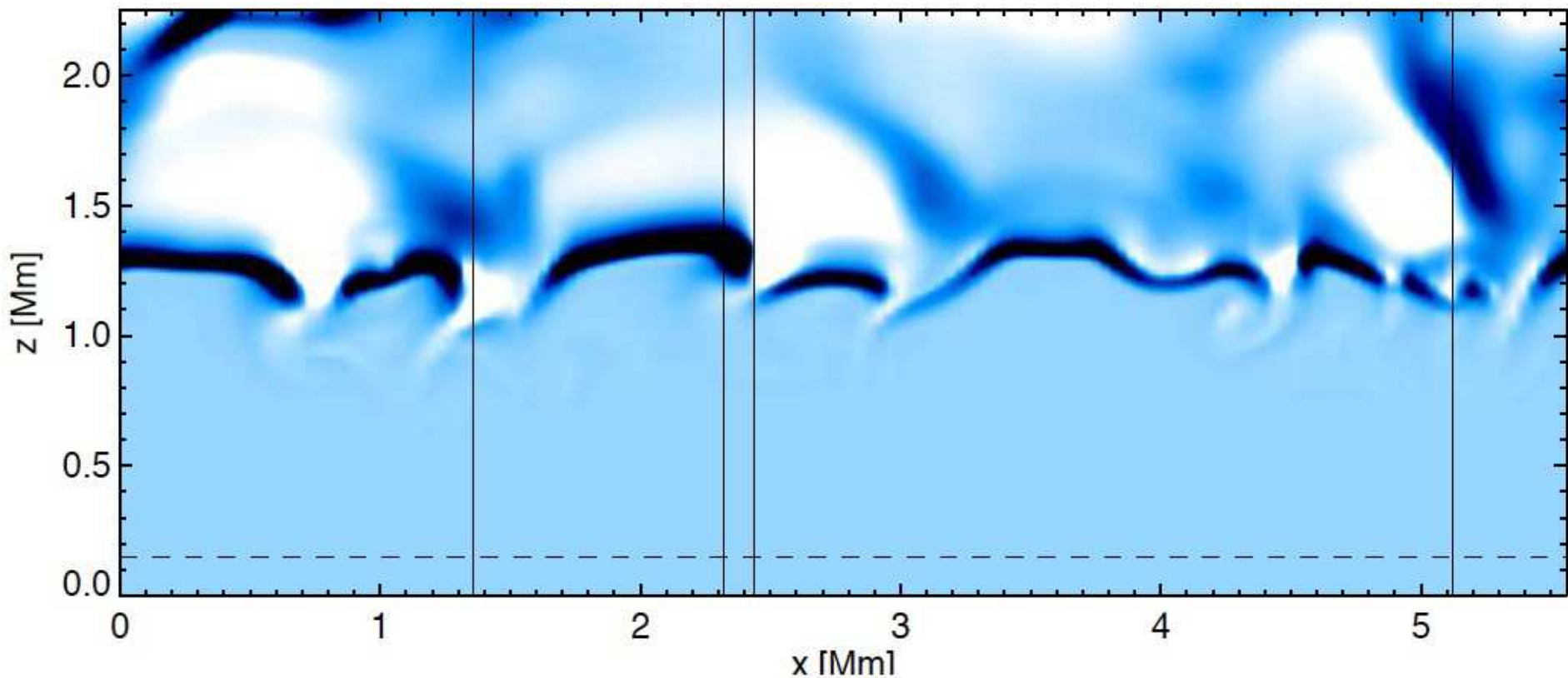


A single flux sheet/tube influences the radiative escape in a cross-sectional area that is much wider than the magnetic field concentration proper.



At heliocentric angle $\mu = 0.54$, the facular size \perp to the limb is $\approx 0.5''$ and more. From *Lites et al. 2004*.

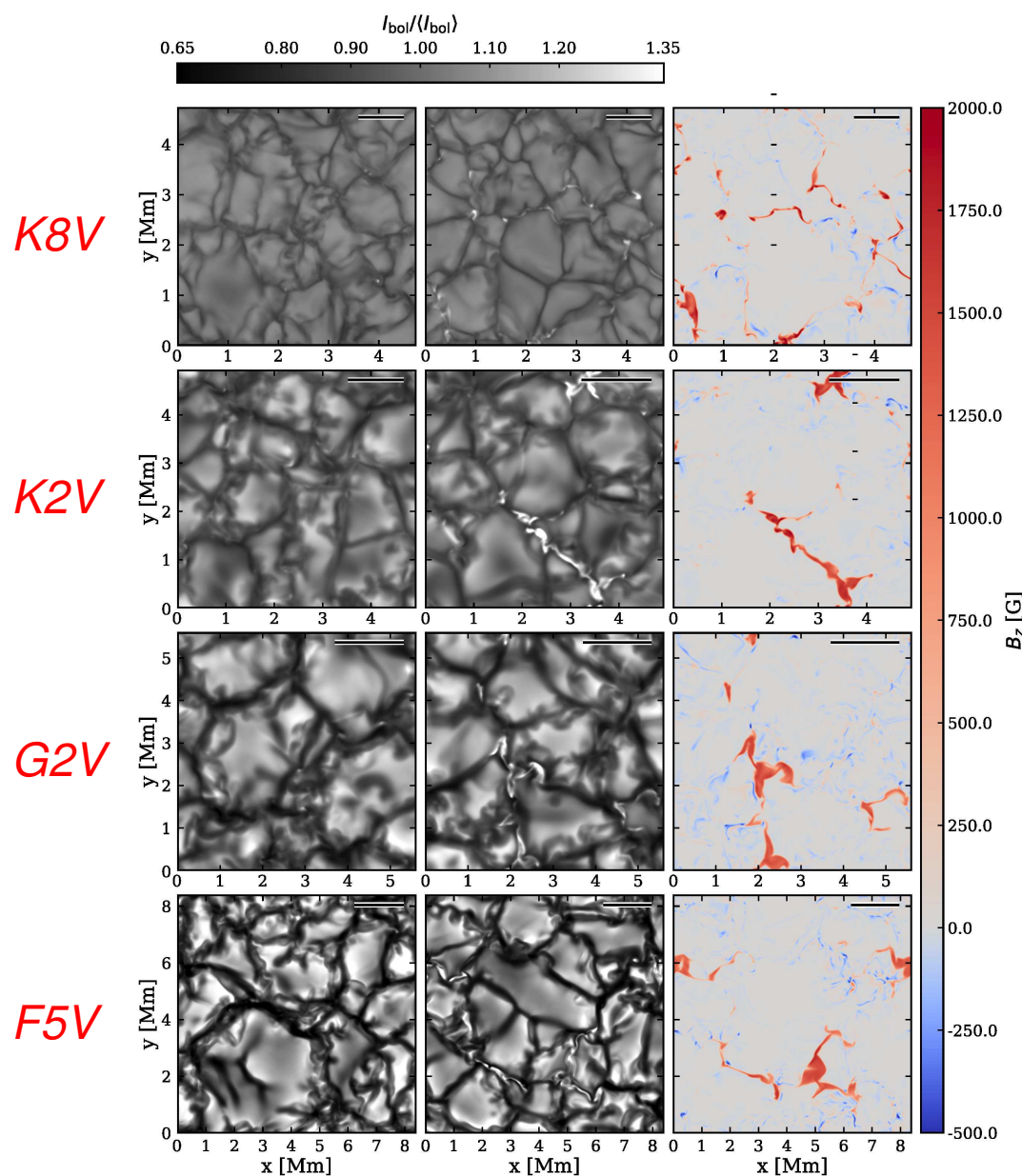
On irradiance (cont.)



Radiative *cooling (dark)* and *heating (bright)* per unit mass, Q_{rad} / ρ , in a vertical slice of a 3-D solar CO^5BOLD model with 12 opacity bins and 4+1 ray inclinations μ .

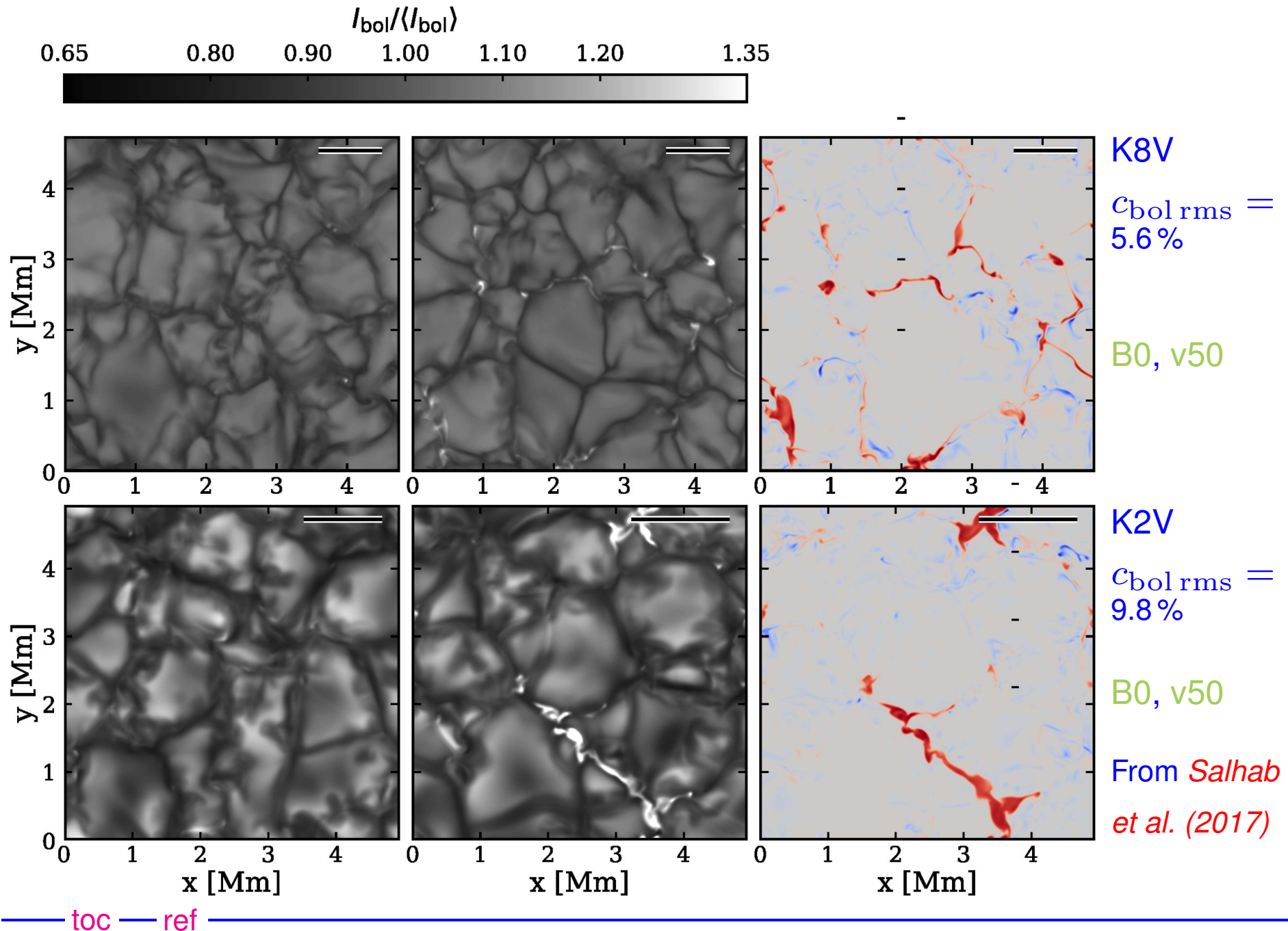
From *Steffen 2017*.

§ 3 Stellar irradiance variability

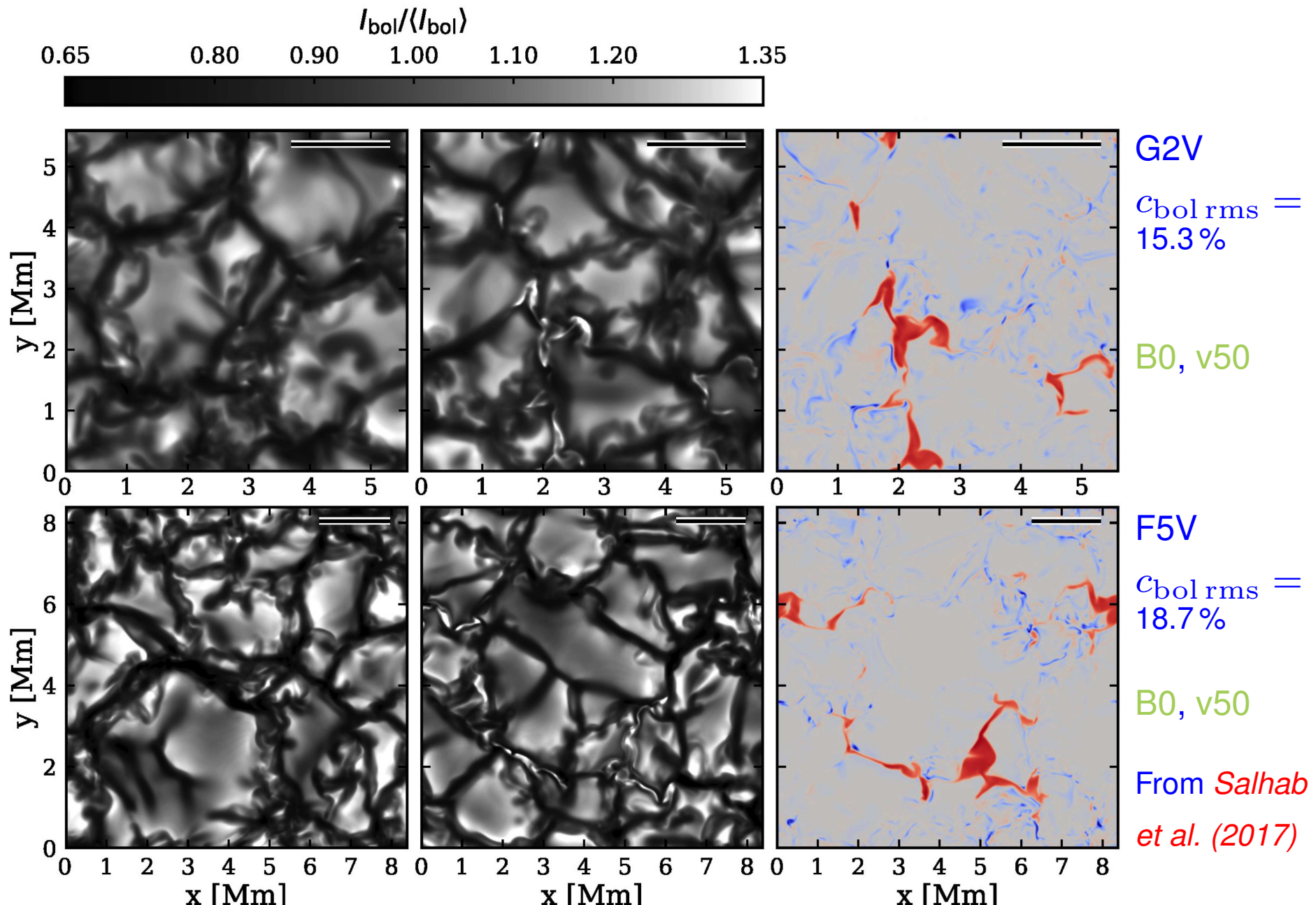


- “*Box in a star*” simulations of the surface layers of four spectral types;
- Each simulation is *run twice*: with and without magnetic fields;
- Initial vertical homogeneous field of *50 G* and *100 G*;
- Multi-group *radiation transfer* using 5 opacity bins;
- Numerical, non-stationary, three-dimensional radiation magnetohydrodynamics using the *CO⁵ BOLD code*.

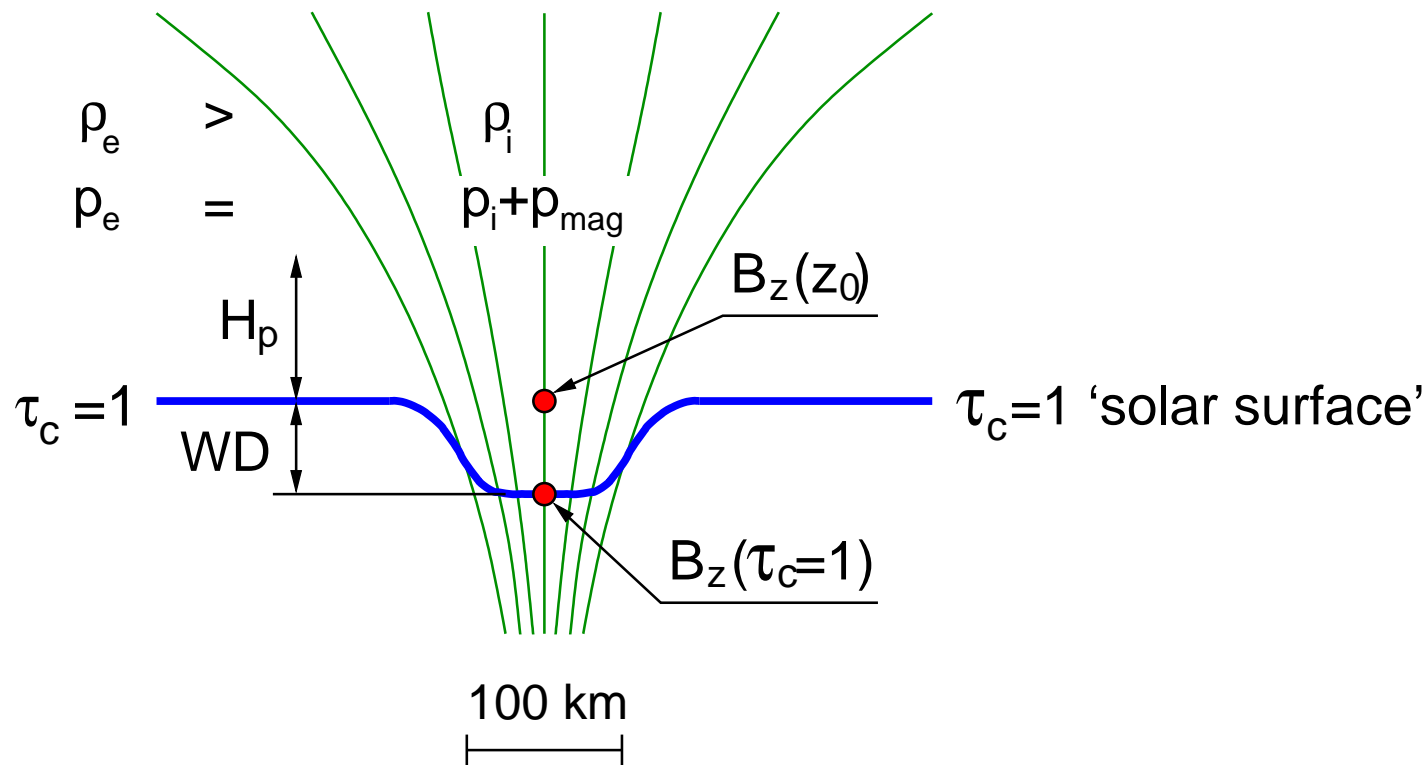
3. Stellar irradiance variability (cont.)



3. Stellar irradiance variability (cont.)



3. Stellar irradiance variability (cont.)

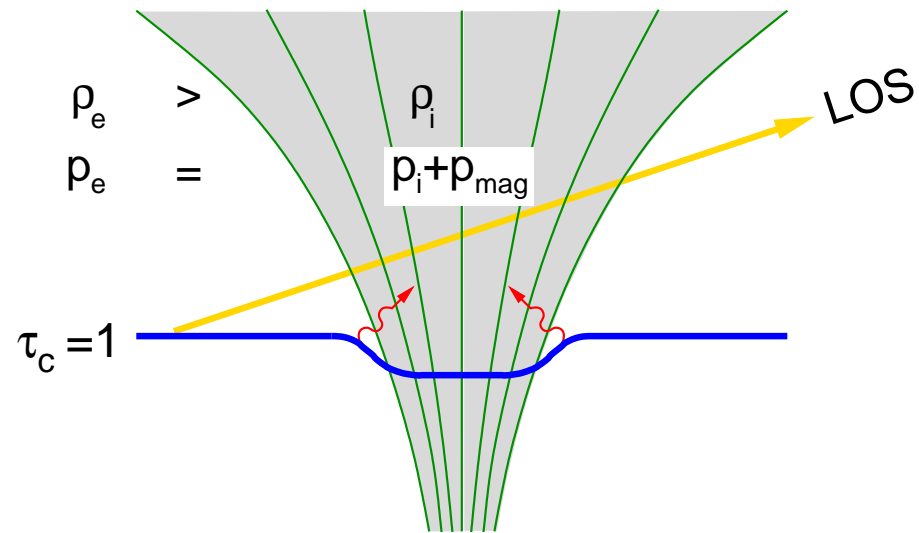


Magnetic flux
concentration
(green) with optical
surface $\tau_c = 1$
(blue), and “Wilson
depression” WD.

Conclusion: $B_z(\tau_R = 1) \approx 1550 [\text{G}]$ is fairly
independent of spectral type

3. Stellar irradiance variability (cont.)

Magnetic flux sheath in a



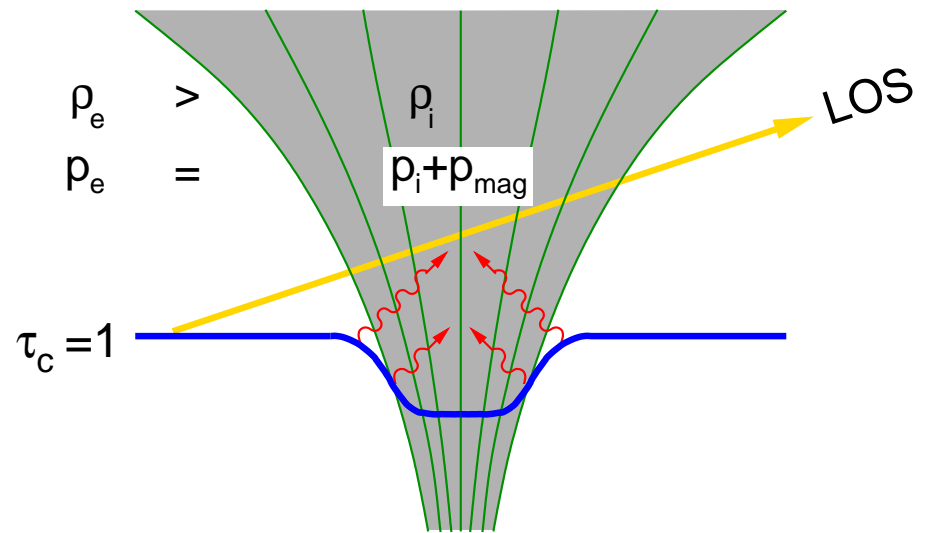
K-type atmosphere

Small depression of the $\tau_c = 1$ surface

\Rightarrow *weak hot-wall effect*.

Weak evacuation

\Rightarrow *faint facular granules*.



G-type atmosphere.

Large depression of the $\tau_c = 1$ surface

\Rightarrow *strong hot-wall effect*.

Strong evacuation

\Rightarrow *bright facular granules*.

3. Stellar irradiance variability (cont.)

	spectral type	K8V	K2V	G2V	F5V
	initial B_z [G]	50	50	50	50
25	δI_{bol} [%]	0.25 ± 0.2	0.68 ± 0.9	0.88 ± 1.1	0.53 ± 0.8
26	δF_{bol} [%]	0.39 ± 0.2	0.86 ± 0.9	1.15 ± 1.1	0.95 ± 0.8
27	$\delta F_{\text{bol}} - \delta I_{\text{bol}}$ [%]	0.14	0.18	0.27	0.42
30	WD _w [km]	60 ± 14	139 ± 34	232 ± 65	388 ± 113
31	$\text{WD}_w / H_p(\tau_R = 1)$ [-]	0.7 ± 0.1	1.3 ± 0.3	1.4 ± 0.3	2.6 ± 0.7
15	$\rho_{\text{int}} / \rho_{\text{ext}}(z_0)$ [-]	0.75 ± 0.02	0.54 ± 0.03	0.46 ± 0.04	0.36 ± 0.05
16	$\beta(z_0)$ [-]	2.7 ± 0.2	1.3 ± 0.1	0.74 ± 0.1	0.38 ± 0.1

Radiative surplus of the magnetic over the field-free models, weighted mean *Wilson depression*, and degree of *evacuation* of the flux concentrations.

3. Stellar irradiance variability (cont.)

Conclusion: For spectral types K8V to F5V, the small-scale magnetic fields produce a *surplus in radiative intensity and flux*. It is most pronounced for G-type and early K-type stars.

Table of content

1. On magnetic flux tubes
2. On irradiance
3. Stellar irradiance variability

References

References

- Solanki, S.K.: 1987, *The Photospheric Layers of Solar Magnetic Fluxtubes*, PhD theis, ETH 8309
- Pneuman, G.W., Solanki, S.K., and Stenflo, J.O.: 1986, *Structure and merging of solar magnetic fluxtubes*, Astron. Astrophys. **154**, 231
- Steiner, O., Pneuman, G.W., and Stenflo, J.O.: 1986, *Numerical models of solar magnetic fluxtubes*, Astron. Astrophys. **170**, 126
- Ferriz Mas, A. and Schüssler, M.: 1989, *Radial expansion of the magnetohydrodynamic equations for axially symmetric configurations*, Geophys. Astrophys. Fluid Dynamics **48**, 217-234
- Steiner, O: 1990, *Model calculations of solar magnetic flux tubes and radiative transfer*, PhD theis, ETH 9292
- Berger, T.E., Rouppe van der Voort, L.H.M., Löfdahl, M.G., Carlsson, M., Fossum, A. Hansteen, V.H., Marthinussen, E., Title, A., and Scharmer, G.: 2004, *Solar magnetic elements at 0.1'' resolution: General appearance and magnetic structure*, Astron. Astrophys. **428**, 613?628
- Rouppe van der Voort, L.H.M., Hansteen1, V.H., Carlsson, M., Fossum, A., Marthinussen, E., van Noort, M.J., and Berger, T.E.: 2005, *Solar magnetic elements at 0.1'' resolution: II. Dynamical evolution*, Astron. Astrophys. **435**, 327-337

References (cont.)

- Vögler, A., Shelyag, S., Schüssler, M., Cattaneo, F., Emonet, T., and Linde, T.: 2005, *Simulations of magneto-convection in the solar photosphere: Equations, methods, and results of the MURaM code*, Astron. Astrophys. **429**, 335-351
- Steiner, O., Salhab, R.G., Freytag, B., Rajaguru, S. P., Schaffenberger, W., and Steffen, M.: 2014, *Properties of small-scale magnetism of stellar atmospheres*, Publ. Astron. Soc. Japan **66**, S5-1
- Salhab, R.G., Steiner, O., Berdyugina, S.V., Freytag, B., Rajaguru, S. P., and Steffen, M.: 2018, *Simulation of the small-scale magnetism in main sequence stellar atmospheres*, Astron. Astrophys. **614**, A78
- Deinzer, W., Hensler, G., Schüssler, M., and Weisshaar, E.: 1984, *Model calculations of magnetic flux tubes: I. Equations and method*, Astron. Astrophys. **139**, 426
- Deinzer, W., Hensler, G., Schüssler, M., and Weisshaar, E.: 1984, *Model calculations of magnetic flux tubes: II Stationary results for solar magnetic elements*, Astron. Astrophys. **139**, 435

References (cont.)

- Lites, B.W. Scharmer, G.B., Berger, T.E., and A.M. Title: 2004, *Three-dimensional structure of the active region photosphere as revealed by high angular resolution*, Solar Phys. **221**, 65-84
- Steffen, M.: 2017, *Radiation transport in CO5BOLD: A short-characteristics module for local box models*, Mem. Soc. Astr. Italiana **88**, 22